Matrix-based formulation of the iterative randomized stimulation and averaging method for recording evoked potentials

Angel de la Torre, Joaquin T. Valderrama, Jose C. Segura, and Isaac M. Alvarez

Citation: The Journal of the Acoustical Society of America **146**, 4545 (2019); doi: 10.1121/1.5139639
View online: https://doi.org/10.1121/1.5139639
View Table of Contents: https://asa.scitation.org/toc/jas/146/6
Published by the Acoustical Society of America

Matrix-based formulation of the iterative randomized stimulation and averaging method for recording evoked potentials

Angel de la Torre,[1] Joaquin T. Valderrama,[2,a)] Jose C. Segura,[1] and Isaac M. Alvarez[1]
[1]*Department of Signal Theory, Telematics, and Communications, University of Granada, Granada, Spain*
[2]*National Acoustic Laboratories, Sydney, Australia*

(Received 4 June 2019; revised 16 October 2019; accepted 15 November 2019; published online 26 December 2019)

The iterative randomized stimulation and averaging (IRSA) method was proposed for recording evoked potentials when the individual responses are overlapped. The main inconvenience of IRSA is its computational cost, associated with a large number of iterations required for recovering the evoked potentials and the computation required for each iteration [involving the whole electroencephalogram (EEG)]. This article proposes a matrix-based formulation of IRSA, which is mathematically equivalent and saves computational load (because each iteration involves just a segment with the length of the response, instead of the whole EEG). Additionally, it presents an analysis of convergence that demonstrates that IRSA converges to the least-squares (LS) deconvolution. Based on the convergence analysis, some optimizations for the IRSA algorithm are proposed. Experimental results (configured for obtaining the full-range auditory evoked potentials) show the mathematical equivalence of the different IRSA implementations and the LS-deconvolution and compare the respective computational costs of these implementations under different conditions. The proposed optimizations allow the practical use of IRSA for many clinical and research applications and provide a reduction of the computational cost, very important with respect to the conventional IRSA, and moderate with respect to the LS-deconvolution. MATLAB/Octave implementations of the different methods are provided as supplementary material.
https://doi.org/10.1121/1.5139639

[BLM] Pages: 4545–4556

I. INTRODUCTION

Evoked response is recorded using electrodes and amplifying the electrical signal associated with the neural activity evoked by a stimulus. Usually, the amplitude of this signal is very low compared to that of the noise (i.e., the signal to noise ratio, SNR, is low), and therefore the evoked potentials are obtained by averaging the responses to a number of stimuli (Thornton, 2007). Synchronized averaging provides an accurate estimate of the response only when the stimuli are adequately separated from each other and there is no overlapping between each individual response and the responses elicited by the adjacent stimuli (Woldorff, 1993). This method constrains the recording of evoked potentials to a minimum interstimulus interval (ISI) equal to the duration of the response. However, recording responses evoked at a high stimulation rate is useful in order to investigate adaptation mechanisms (i.e., how the responses are affected by the stimulation rate) (Gillespie and Muller, 2009; Thornton and Coleman, 1975), particularly because in normal perception, stimuli are not presented in an isolated or quasi-isolated way.

There are several procedures proposed for recording auditory evoked potentials (AEPs) at high stimulation rates. The most relevant methods are maximum length sequences (MLS) (Eysholdt and Schreiner, 1982; Thornton and Slaven, 1993), adjacent-responses (ADJAR) (Woldorff, 1993), quasi-periodic sequence deconvolution (QSD) (Jewett *et al.*, 2004), continuous loop averaging deconvolution (CLAD) (Bohorquez and Ozdamar, 2006; Ozdamar and Bohorquez, 2006), randomized stimulation and averaging (RSA) (Valderrama *et al.*, 2012), and least-squares (LS) deconvolution (Bardy *et al.*, 2014a; Bardy *et al.*, 2014b; Bardy *et al.*, 2014c; Maddox and Lee, 2018). What these methods have in common is that the ISI is not constant (otherwise, the interference associated with overlapping cannot be avoided).

Among them, RSA allows a flexible design of the ISI distribution (Valderrama *et al.*, 2012), which is particularly useful for investigating several adaptation phenomena (Valderrama *et al.*, 2014c). Even though RSA provides the evoked potentials when the responses are overlapped (i.e., when the ISI is shorter than the duration of the response), Valderrama *et al.* (2014b) demonstrated that the recovered response is affected by distortion depending on the ISI distribution and the autocorrelation function of the response. Particularly, a narrow distribution of ISI causes a strong distortion of the recovered response. For example, the increased magnitude response reported in the 40 Hz steady-state response is the result of a constructive interference associated with the aforementioned distortion (Bohorquez and Ozdamar, 2008; Galambos *et al.*, 1981). An iterative version of RSA (called iterative-randomized stimulation and averaging, or IRSA) was proposed in order to minimize this distortion and provide a more accurate estimate of the response (Valderrama *et al.*, 2014b). In IRSA, the algorithm is initialized with the response provided by synchronized average

a)Also at: Department of Linguistics, Macquarie University, Sydney, Australia. Electronic mail: joaquin.valderrama@nal.gov.au

using RSA. Using this initial estimation of the evoked response, the expected electroencephalogram (EEG), i.e., the convolution of the stimulation sequence with the estimated response, is subtracted from the recorded EEG, and the residual EEG is averaged in order to estimate a correction to the response. The corrected response is then used to update the expected EEG, and the new residual EEG is averaged to estimate a new correction, and the process iteratively repeated until convergence.

IRSA was demonstrated to be a strong algorithm to recover responses evoked at high stimulation rates because it provides non-distorted responses even for restrictive ISI distributions, which provides a lot of flexibility in the experimental design. However, IRSA presents two important inconveniences. The first one is that, sometimes, the algorithm solution tends to oscillate, depending on the statistical properties of the stimulation sequence. Particularly, narrow distributions of the ISI increase the risk of oscillation. The oscillations can easily be avoided by including a convergence control parameter (α) in the algorithm, representing the relative updating performed at each iteration. A small enough α avoids oscillations, but in this case, IRSA requires a larger number of iterations to converge. The second inconvenience is the amount of computation involved in the IRSA algorithm (particularly when α is small and therefore many iterations are required): each iteration requires the manipulation of the whole EEG (in order to estimate the residual EEG), and therefore the computational load of IRSA is prohibitive in most practical applications.

The IRSA method has been successfully applied in several AEP experiments, showing its potential with respect to the flexibility in the stimulation design (Burkard *et al.*, 2018; Finneran, 2017, 2018; Finneran *et al.*, 2019; Valderrama *et al.*, 2014c; Valderrama *et al.*, 2016). However, despite its advantages, IRSA is not extensively applied due to the associated computational load, and its utilization has been limited to experimental configurations in which the algorithm complexity is not very restrictive (i.e., evoked responses with short duration, as in the case of auditory brainstem responses).

In this article we propose a matrix-based formulation aiming to reduce the computational complexity of the IRSA method. This formulation is mathematically equivalent to the conventional one but provides a significant reduction of the computational load. Additionally, we present a convergence analysis of the matrix-IRSA method which demonstrates that IRSA converges to the LS-deconvolution method (Bardy *et al.*, 2014a; Bardy *et al.*, 2014b; Bardy *et al.*, 2014c), also proposed for recovering evoked responses at high stimulation rate. Using real EEGs recorded in an AEP experiment, several versions of the IRSA (including different optimizations) and LS-deconvolution methods are compared in order to demonstrate the mathematical equivalence and to evaluate their respective computational costs.

II. MATRIX FORMULATION OF IRSA

A. EEG model

The digital EEG $y(n)$ acquired in an AEP recording procedure is usually modeled as a convolutional process (Jewett *et al.*, 2004; Ozdamar and Bohorquez, 2006)

$$y(n) = s(n) * x(n) + n_0(n), \tag{1}$$

where n is the index of the samples; N is the number of samples of the EEG ($n \in \{0, \ldots, N-1\}$); $s(n)$ is the stimulation sequence consisting of one impulse at the beginning of each stimulation event; $x(n)$ represents the evoked response to each stimulus [with $x(n)$ null for $n > (J-1)$, J being the length of the evoked response]; $n_0(n)$ represents the noise affecting the EEG; and the asterisk ($*$) represents convolution. If the stimulation sequence contains K events at the samples m_k, the stimulation sequence can be written as

$$s(n) = \sum_{k=0}^{K-1} \delta(n - m_k), \tag{2}$$

where $\delta(n)$ is the unitary impulse at $n = 0$. Taking into account that $x(n) * \delta(n - m_k) = x(n - m_k)$, the EEG can be rewritten as

$$y(n) = \sum_{k=0}^{K-1} x(n - m_k) + n_0(n). \tag{3}$$

B. RSA and IRSA procedures

The RSA determination of the evoked response provides an estimate of the response by synchronous averaging of the EEG (Valderrama *et al.*, 2012)

$$\hat{x}(j) = \frac{1}{K} \sum_{k=0}^{K-1} y(j + m_k), \tag{4}$$

with $j \in \{0, \ldots, J-1\}$. When the length of the response J (i.e., the number of samples for which the response can be assumed to be non-null) is smaller than the minimum ISI, this estimation is only affected by the noise, and averaging with a large enough number of stimuli provides an accurate estimate of the response. However, if the responses are overlapped (the minimum ISI is smaller than J), the interference associated with adjacent responses degrades the estimation.

The IRSA algorithm aims to overcome the effect of this interference. The main idea of IRSA is that the interference can be estimated using the estimated response $\hat{x}(j)$, and therefore, a more accurate response can iteratively be estimated by averaging a modified EEG in which the interference associated with the adjacent responses is suppressed (Valderrama *et al.*, 2014b; Valderrama *et al.*, 2016). By using the estimated response at iteration i, $\hat{x}_i(j)$, an interference-free EEG for the kth stimulus (i.e., in which the interference from all the stimuli except the kth is suppressed) can be derived as

$$y_{k,i}(n) = y(n) - \sum_{k'=0, k' \neq k}^{K-1} \hat{x}_i(n - m_{k'}), \tag{5}$$

and the evoked response can be estimated at iteration $i+1$ by averaging the EEG portions without interference

$$\hat{x}_{i+1}(j) = \frac{1}{K} \sum_{k=0}^{K-1} y_{k,i}(j + m_k). \tag{6}$$

This way, each iteration provides a better estimate of the evoked response, which also leads to a more accurate suppression of the interference for the next iteration. Through this iterative process, IRSA tends to minimize the effect of the interference caused by overlapping responses.

In general, an evoked-potential recording session involves a large number of stimuli and a long EEG. Therefore, the proposed IRSA is unpractical, because, at each iteration i, K EEGs should be calculated (each one including only the kth response and suppressing all the others), leading to a large amount of computation. However, the computation can be simplified, since suppressing all except one is equivalent to suppress all and then add one

$$\begin{aligned} y_{k,i}(n) &= y(n) - \sum_{k'=0}^{K-1} \hat{x}_i(n - m_{k'}) + \hat{x}_i(n - m_k) \\ &= r_i(n) + \hat{x}_i(n - m_k), \end{aligned} \tag{7}$$

where $r_i(n) = y(n) - s(n) * \hat{x}_i(n)$ represents the residual of the EEG, i.e., the recorded EEG minus the EEG expected from the estimated response $\hat{x}_i(j)$ and the stimulation sequence $s(n)$. With this definition, the IRSA estimation can be reformulated as

$$\begin{aligned} \hat{x}_{i+1}(j) &= \frac{1}{K}\sum_{k=0}^{K-1} r_i(j + m_k) + \frac{1}{K}\sum_{k=0}^{K-1} \hat{x}_i(j - m_k + m_k) \\ &= \frac{1}{K}\sum_{k=0}^{K-1} r_i(j + m_k) + \hat{x}_i(j), \end{aligned} \tag{8}$$

or if we define $z_i(j)$ as the averaged residual

$$z_i(j) = \frac{1}{K}\sum_{k=0}^{K-1} r_i(j + m_k), \tag{9}$$

the iterative estimation of the response can be written as

$$\hat{x}_{i+1}(j) = z_i(j) + \hat{x}_i(j). \tag{10}$$

Even though the IRSA algorithm usually converges to a stable solution, it was found that it is sometimes unstable, depending on the distribution of ISI in the stimulation sequence. This instability produces an oscillation of the solution from iteration to iteration (Valderrama *et al.*, 2014b). The risk of instability particularly increases for narrow ISI distributions. Including a convergence control parameter (α, in the range [0,1]) was found to be a simple solution in order to avoid this instability,

$$\hat{x}_{i+1}(j) = \hat{x}_i(j) + \alpha \cdot z_i(j). \tag{11}$$

According to Valderrama *et al.* (2014b), a small enough α guarantees convergence and stability of IRSA, but requires more iterations to reach convergence.

Taking into account the previous derivations, the conventional IRSA algorithm can be summarized as follows:

(1) Initialization

$$\hat{x}_0(j) = 0 \quad z_0(j) = \frac{1}{K}\sum_{k=0}^{K-1} y(j + m_k). \tag{12}$$

(2) Response updating

$$\hat{x}_i(j) = \hat{x}_{i-1}(j) + \alpha \cdot z_{i-1}(j). \tag{13}$$

(3) Residual estimation

$$r_i(n) = y(n) - \sum_{k=0}^{K-1} \hat{x}_i(n - m_k). \tag{14}$$

(4) Averaged-residual estimation

$$z_i(j) = \frac{1}{K}\sum_{k=0}^{K-1} r_i(j + m_k). \tag{15}$$

(5) Steps 2–4 are repeated until convergence.

In this algorithm, $j = 0,\ldots,J-1$ in steps 1, 2, and 4, and $n = 0,\ldots,N-1$ in step 3.

The energy of the averaged residual tends to decrease with the iterations, and different convergence criteria can be applied (for example, a minimum reduction of the averaged residual energy, a relative reduction of the averaged residual energy with respect to that of the previous iteration, a predefined number of iterations, etc.).

It can be noted that $z_0(j)$ in IRSA corresponds to the estimation provided by RSA [in Eq. (4)]. The computational complexity increases linearly with the number of iterations and is also influenced by the EEG length (N) because of Eq. (14) and the product of the response length times the number of stimuli ($J \times K$) because of Eqs. (14) and (15). The computational cost associated with Eq. (13) is negligible compared to that of the other equations. Therefore, the computational complexity of IRSA is prohibitive in situations with a large number of stimuli (and therefore a long EEG) and/or requiring a large number of iterations. This makes conventional IRSA difficult to be applied or unpractical in most applications. The supplementary material[1] (section 1) includes MATLAB/Octave code implementing the IRSA algorithm.

C. Matrix representation of the IRSA procedure

The signals involved in the convolutional model of the EEG [$y(n)$, $s(n)$, $x(j)$ and $n_0(n)$] and Eq. (1) can be represented using a matrix notation

$$\mathbf{y} = S\mathbf{x} + \mathbf{n}_0, \tag{16}$$

where $\mathbf{y}$, $S\mathbf{x}$, and $\mathbf{n}_0$ are N-component column vectors (representing the EEG signal, the convolution of the stimulation signal with the response and the noise, respectively), $\mathbf{x}$ is a J-component column vector and S is a $N \times J$ matrix (with N rows and J columns) with $S(n,j) = s(n-j)$ providing the convolution $s(n) * x(n)$ as a matrix operation. It should be noted that $s(n)$ is null for all the samples except for those corresponding to the stimulation events (at samples m_k), and therefore, most of the elements in the stimulation matrix S are null.

Similarly, Eq. (4) can be rewritten in matrix notation as

$$\hat{\mathbf{x}} = \frac{1}{K} S^T \mathbf{y} = S_K \mathbf{y} \quad S_K \equiv \frac{1}{K} S^T, \tag{17}$$

where S^T is the transposed of matrix S, and S_K is defined from S including transposition and normalization. The last equation provides the RSA solution in matrix notation. With these definitions, IRSA can easily be formulated with matrix notation as follows:

(1) Initialization: $\hat{\mathbf{x}}_0 = 0; \quad \mathbf{z}_0 = S_K \mathbf{y}.$ (18)

(2) Response estimation: $\hat{\mathbf{x}}_i = \hat{\mathbf{x}}_{i-1} + \alpha \mathbf{z}_{i-1}.$ (19)

(3) Residual estimation: $\mathbf{r}_i = \mathbf{y} - S\hat{\mathbf{x}}_i.$ (20)

(4) Averaged-residual estimation: $\mathbf{z}_i = S_K \mathbf{r}_i.$ (21)

(5) Steps 2 to 4 repeated until convergence.

Using this matrix notation, it can be observed that steps 3 and 4 can be compacted in one step

$$\mathbf{z}_i = S_K \mathbf{r}_i = S_K \mathbf{y} - S_K S \hat{\mathbf{x}}_i = \mathbf{z}_0 - R_s \hat{\mathbf{x}}_i, \tag{22}$$

where R_s is a $J \times J$ square matrix resulting of the product of matrices S_K and S. Taking into account its definition, the matrix R_s is the normalized autocorrelation matrix of the stimulation sequence $s(n)$, and can also be obtained as

$$R_s(j_1, j_2) = \frac{1}{K} r_s(|j_1 - j_2|) \quad \forall j_1, j_2 \in \{0, \ldots, J-1\}, \tag{23}$$

where $r_s(j)$ is the autocorrelation function of $s(n)$

$$r_s(j) = \sum_{n=j}^{N-J} s(n)s(n+j) \quad \forall j = 0, \ldots, J-1, \tag{24}$$

and, as all the autocorrelation matrices, R_s is a Toeplitz-symmetric positive semidefinite matrix [all the elements are identical in each direct diagonal, $R_s(j_1, j_2) = R_s(j_2, j_1)$, and all the eigenvalues are non-negative].

The proposed combination of steps 3 and 4 using Eq. (22) provides an important reduction of the computational complexity of IRSA. In the conventional IRSA, step (3) requires an operation involving all the EEG and all the stimuli in order to calculate $r_i(n)$, and step (4) requires an operation involving the full $r_i(n)$ signal (with the same duration of the EEG) and all the stimuli. In contrast, the matrix based formulation of IRSA does not require calculating $r_i(n)$ since $z_i(j)$ is directly estimated from $z_0(j)$, $r_s(j)$, and $\hat{x}_i(j)$. Additionally, the estimation of $z_i(j)$ only involves the matrix operation $R_s \hat{\mathbf{x}}_i$ with a $J \times J$ matrix, and a summation of vectors with J elements, where the vector $\mathbf{z}_0$ and the matrix R_s are used in all iterations (and therefore, they can be computed just once at the beginning of the algorithm).

With these considerations in mind, the matrix implementation of the IRSA algorithm is the following:

(1) Initialization

$$\hat{x}_0(j) = 0 \quad z_0(j) = \frac{1}{K} \sum_{k=0}^{K-1} y(j + m_k)$$

$$r_s(j) = \sum_{n=j}^{N-J} s(n)s(n-j) \quad \{\hat{\mathbf{x}}_0, \mathbf{z}_0, R_s\}. \tag{25}$$

(2) Response updating

$$\hat{\mathbf{x}}_i = \hat{\mathbf{x}}_{i-1} + \alpha \mathbf{z}_{i-1}. \tag{26}$$

(3) Averaged-residual estimation

$$\mathbf{z}_i = \mathbf{z}_0 - R_s \hat{\mathbf{x}}_i. \tag{27}$$

(4) Steps 2 and 3 are repeated until convergence.

According to the proposed formulation, the matrix implementation of the IRSA algorithm requires an initialization (where two J-dimension vectors, $\hat{\mathbf{x}}_0$ and $\mathbf{z}_0$, and a $J \times J$ matrix R_s are estimated) and an iterative procedure, involving matrix and vector operations in a J-dimensional space. It should be noted that the matrix implementation of IRSA is mathematically equivalent to the conventional IRSA. However, the computational complexity is substantially smaller because there are computations involving the whole EEG only at initialization (i.e., estimation of $\mathbf{z}_0$ and R_s), and the computations at the iterations just involve matrix or vector operations with dimensionality J. In other words, the computational complexity of the iterations depends on the length of the response (J), but neither on the length of the EEG (N) nor on the number of stimuli (K). This provides a very efficient implementation of the IRSA algorithm even for experiments with a large number of stimuli or long EEGs. The supplementary material[1] (section 2) includes MATLAB/Octave code implementing the matrix IRSA algorithm.

D. Convergence of the IRSA algorithm

The matrix formulation of the IRSA algorithm allows an analysis of converge. If $\hat{\mathbf{x}}_i$ in Eq. (27) is substituted by Eq. (26), we obtain

$$\mathbf{z}_i = \mathbf{z}_0 - R_s(\hat{\mathbf{x}}_{i-1} + \alpha \mathbf{z}_{i-1}), \tag{28}$$

and taking into account that, according to Eq. (27), $\mathbf{z}_0 - R_s \hat{\mathbf{x}}_{i-1} = \mathbf{z}_{i-1}$, a new recursion is obtained

$$\mathbf{z}_i = \mathbf{z}_{i-1} - \alpha R_s \mathbf{z}_{i-1} = (I - \alpha R_s)\mathbf{z}_{i-1}, \tag{29}$$

where I is the $J \times J$ identity matrix. This recursion provides the averaged residual at an arbitrary iteration

$$\mathbf{z}_i = (I - \alpha R_s)^i \mathbf{z}_0. \tag{30}$$

Similarly, the response estimation can be obtained as

$$\hat{\mathbf{x}}_1 = \alpha \mathbf{z}_0, \tag{31}$$

$$\hat{\mathbf{x}}_2 = \alpha \mathbf{z}_0 + \alpha \mathbf{z}_1 = \alpha \mathbf{z}_0 + \alpha(I - \alpha R_s)\mathbf{z}_0, \tag{32}$$

$$\hat{\mathbf{x}}_3 = \alpha \mathbf{z}_0 + \alpha(I - \alpha R_s)\mathbf{z}_0 + \alpha(I - \alpha R_s)^2 \mathbf{z}_0 \ldots \tag{33}$$

and the estimation at the ith iteration is

$$\hat{\mathbf{x}}_i = \sum_{j=0}^{i-1} \alpha(I - \alpha R_s)^j \mathbf{z}_0 = \alpha \left(\sum_{j=0}^{i-1} (I - \alpha R_s)^j \right) \mathbf{z}_0, \quad (34)$$

where the sum is a geometric series of matrices. The solution of the geometric series provides a direct estimation of the response at iteration i (detailed derivations are included in the supplementary material,[1] section 3)

$$\hat{\mathbf{x}}_i = (I - (I - \alpha R_s)^i) R_s^{-1} \mathbf{z}_0, \quad (35)$$

where R_s^{-1} is the inverse of the autocorrelation matrix R_s (which requires that R_s can be inverted, i.e., that all its eigenvalues are non-null). If the absolute values of all the eigenvalues of $(I - \alpha R_s)$ are smaller than 1, the geometrical series converges to $(\alpha R_s)^{-1}$, and therefore the IRSA estimation converges to

$$\hat{\mathbf{x}}_\infty = \lim_{i \to \infty} \hat{\mathbf{x}}_i = R_s^{-1} \mathbf{z}_0. \quad (36)$$

This is not a surprising result since averaging of the convolutional model in Eq. (16) is

$$S_k \mathbf{y} = S_k S \mathbf{x} + S_k \mathbf{n}_0, \quad (37)$$

or, equivalently

$$\mathbf{z}_0 = R_s \mathbf{x} + S_k \mathbf{n}_0, \quad (38)$$

and if R_s is non singular (and can, therefore, be inverted), this equation can be rewritten as

$$\mathbf{x} = R_s^{-1} \mathbf{z}_0 - R_s^{-1} S_k \mathbf{n}_0. \quad (39)$$

In this equation, the contribution of the noise is usually small, since it decreases as the duration of the EEG increases because of the averaging effect of S_k. If the contribution of the noise is ignored, this equation provides the least squares estimation of the response (Bardy *et al.*, 2014a; Bardy *et al.*, 2014b; Bardy *et al.*, 2014c)

$$\hat{\mathbf{x}}_{LS} = R_s^{-1} \mathbf{z}_0. \quad (40)$$

This new perspective of the IRSA formulation leads to several relevant implications. Regarding the convergence parameter, it can be demonstrated that the convergence condition requires that $\alpha < 2/\max(\mu_j)$, where μ_j are the eigenvalues of the autocorrelation matrix R_s (detailed demonstration is included in the supplementary material, section 3.5).[1] This condition explains why a too large convergence parameter produces instability and oscillations of the IRSA solution, and why low-jittered stimulation sequences (with resonances in the autocorrelation function and large eigenvalues in the autocorrelation matrix) require a smaller convergence parameter and more iterations, as observed in previous studies (Valderrama *et al.*, 2016). This condition also provides a criterion for selecting an appropriate convergence parameter based on the eigenvalues of R_s.

Additionally, the inversion of the autocorrelation matrix R_s directly provides the IRSA solution at convergence with neither the iterative procedure nor the convergence parameter α. In other words, the number of iterations and the convergence parameter (that should be carefully configured in IRSA for a given stimulation configuration in order to avoid instability and guarantee convergence) become irrelevant with the LS estimation and, therefore, the computational cost of this alternative is associated to the initialization and the matrix inversion of R_s (but the computational cost associated to the iterations is saved since there are no iterations).

Finally, the convergence analysis of IRSA can be considered a formal demonstration of the equivalence of IRSA (at convergence) and the LS deconvolution procedure proposed by Bardy *et al.* (2014a), Bardy *et al.* (2014b), and Bardy *et al.* (2014c).

E. Considerations related to computational cost

There are several alternatives for the numerical implementation of the different proposed algorithms (conventional IRSA, matrix IRSA, and matrix-inversion based solution), which can strongly affect the computational cost of the procedures. These are discussed in this section.

Regarding the initialization, the initial averaged residual $[z_0(j)]$ and the autocorrelation of the stimulation sequence $[r_s(j)]$ can alternatively be calculated either as correlations or as sums for each impulse of the stimulation sequence. In the first case, the initialization involves all the samples of the stimulation sequence $s(n)$ or the EEG $y(n)$, while in the second case, it just involves a sum of K terms (one for each impulse in the stimulation sequence) for each sample j in the response

$$z_0(j) = \frac{1}{K} \sum_{n=j}^{N-J} s(n) y(n+j) = \frac{1}{K} \sum_{k=0}^{K-1} y(j + m_k), \quad (41)$$

$$r_s(j) = \sum_{n=j}^{N-J} s(n) s(n+j) = \sum_{k=0}^{K-1} s(j + m_k). \quad (42)$$

Taking into account that the number of impulses in the stimulation sequence is always substantially smaller than the number of samples of the EEG (because the stimulation sequence consists of a set of isolated unitary impulses), the second alternative is computationally more efficient. The supplementary material[1] (section 4) includes MATLAB/Octave code implementing the matrix IRSA algorithm with the optimized initialization.

Second, since the autocorrelation matrix is Toeplitz, the matrix product $R_s \hat{\mathbf{x}}_i$ can efficiently be implemented in the frequency domain. Circulant matrices are diagonalized by the discrete Fourier transform (DFT), and performing the matrix product in a domain where the matrix is diagonal simplifies the computation. However, the autocorrelation matrix R_s is Toeplitz, but not circulant, and therefore, the implementation of the matrix product in the frequency domain requires some additional steps: (i) the $J \times J$ Toeplitz matrix R_s has to be extended to obtain a $2J \times 2J$ circulant

matrix C; (ii) the vector to be multiplied $\hat{\mathbf{x}}_i$ has to be zero-padded to obtain a vector with $2J$ components $\hat{\mathbf{x}}_{\mathbf{e}i}$; (iii) the DFT of the first row of the extended matrix and that of the extended vector have to be multiplied (product is performed in the frequency domain); (iv) the inverse DFT applied to the product provides the result in the time domain; and (v) the result in the time domain must be truncated to the first J samples. The DFT can be implemented with the more efficient fast Fourier transform (FFT) algorithm and, since the matrix coefficients and vector components are real, the imaginary part of the result (usually not null due to numerical precision) should be discarded. The supplementary material[1] (section 5) includes some details about matrix product involving Toeplitz matrices performed in the frequency domain and also includes MATLAB/Octave code implementing the matrix IRSA algorithm where the matrix product $R_s\hat{\mathbf{x}}_i$ is performed with an FFT-based computation (section 6). It is interesting to note that the IRSA algorithm cannot be fully implemented in the frequency domain because at each iteration a truncation has to be applied (in order to appropriately compute the matrix product), and this truncation in the time domain requires either an IFFT, a truncation and an FFT or, alternatively, a circular convolution in the frequency domain with the Fourier transform of the truncating window. The first option (more efficient) has been selected for the algorithm implementation.

The convergence parameter α is critical for the optimization of the IRSA algorithm. A small enough value has to be selected in order to avoid instability of the algorithm, but a too small α leads to a slow convergence (requiring more iterations). The convergence condition $[\alpha < 2/\max(\mu_j)$, being μ_j the eigenvalues of $R_s]$ provides a criterion for selecting an appropriate α, but requires the estimation of the eigenvalues, which is expensive in terms of computational cost. However, since R_s is a symmetric Toeplitz matrix, the relation between R_s and the corresponding extended circulant matrix C provides a bound for the eigenvalues of R_s (Ferreira, 1994)

$$\max(\mu_j) < \frac{1}{2}\left(\max_{0\le j'<J}(\lambda_{2j'}) + \max_{0\le j'<J}(\lambda_{2j'+1})\right), \tag{43}$$

where $\lambda_{2j'}$ and $\lambda_{2j'+1}$ are respectively the even and odd eigenvalues of the matrix C that can easily be computed as the FFT of the first row of C. A fast version of the IRSA algorithm has been implemented using a 95% of the maximum value suggested by this bound as convergence parameter α (see the supplementary material,[1] section 7, for details about the eigenvalues of R_s).

Regarding the number of iterations, the algorithm tends to reduce the average residual $\mathbf{z}_i$ up to the numerical precision. For a detailed study of equivalence among the different versions of the IRSA algorithm, exploring the accuracy at numerical convergence is interesting (in the 64 bits floating-point representation, 52 bits are devoted to numerical accuracy, which provides a precision close to 1 in 10^{15}, and therefore the SNR associated to numerical error is around 300 dB). However, for practical purposes involving evoked responses, the accuracy in the estimated response is limited by the noise in the EEG and numerical accuracy beyond 40 dB or 60 dB makes no sense. In order to save unnecessary computation, the fast implementation of the IRSA algorithm estimates, at each iteration, the SNR associated with the algorithm precision (from the averaged residual $\mathbf{z}_i$), and if the SNR is better than a predefined limit, the iterative process stops. The supplementary material[1] (section 8) includes MATLAB/Octave code implementing the fast version of the matrix IRSA algorithm (including the numerical accuracy checking, the optimized convergence parameter, the optimized initialization, and the FFT-based matrix product).

Finally, the matrix-inversion based solutions of the IRSA algorithm have also been implemented. The solution of the geometric series of matrices at iteration i has been implemented for comparing the accuracy with the IRSA algorithms at a given iteration. The solution of the geometric series at convergence (just requiring the inversion of the matrix R_s, i.e., directly providing the LS solution) has been implemented for comparing both the numerical accuracy and the computational cost with the fastest implementation of IRSA at convergence. Since the last algorithm does not involve any iteration and directly provides the LS-deconvolution solution, it is referred to as "randomized stimulation with LS-deconvolution" (RSLSD). It is remarkable that the iterative version of RSLSD is computationally more expensive than the direct RSLSD (since both require matrix inversion but the former also requires iterative matrix products), and therefore the practical interest of the iterative RSLSD is very limited. Matrix inversion, required in both RSLSD algorithms, cannot be performed in the FFT domain, because in general, the matrix R_s is Toeplitz but not circulant. In the iterative version, the matrix product involving the Toeplitz matrix $(I - \alpha R_s)$ could be performed with an FFT-based procedure, but it has not been implemented due to the lack of practical interest of this version. In both versions, when possible, matrix products and matrix inversion have been implemented without explicit computation of the involved matrices (using matrix left division instead of computing the inverse of the matrix, or computing matrix-vector products instead of matrix-matrix products) in order to save computational time and memory requirements. The supplementary material[1] (sections 9 and 10) includes MATLAB/Octave code implementing the RSLSD algorithms at convergence (i.e., for infinite iterations), and for a specified number of iterations, respectively.

III. EXPERIMENTAL RESULTS

A. Experimental design

The proposed matrix implementations of the IRSA algorithm have been evaluated in terms of the mathematical equivalence with respect to the conventional IRSA and in terms of their respective computational efficiencies (using the execution time for comparisons, since this is the most limiting factor in the algorithm computation). This evaluation was based on an AEP experiment, using real EEG recordings, with six different stimulation rates ranging between 1.39 and 44.44 Hz. The ISI of the stimulation signal followed a uniform distribution within an ISI interval

ranging between 15–30 ms (for average stimulation rate 44.44 Hz) and 480–960 ms (for 1.39 Hz). The duration of the experiment for each ISI configuration was 684 s (and therefore, the number of stimuli used for each configuration increased with the stimulation rate). Table I summarizes the configurations involved in the AEP recording session.

The auditory stimulation consisted of a sequence of rarefaction clicks (with a pulse duration of 0.1 ms) presented at the instants defined by the stimulation sequence. The clicks were delivered diotically through ER-3A insert earphones (providing a flat response in the frequency range 0–4 kHz) at 74 dB (hearing level). The recording electrodes were located at the upper forehead (Fz, active), at the right mastoid (Tp10, reference), and at the middle forehead (Fpz, ground). The EEGs were recorded using an instrumentation pre-amplifier, with a (1–3500) Hz bandwidth and 70 dB gain (Valderrama *et al.*, 2013; Valderrama *et al.*, 2014a; Valderrama *et al.*, 2014c) and digitized at a sampling rate of 44 100 Hz with 16 bits/sample. The EEGs were recorded for 684 s at each ISI configuration, resulting in a total EEG duration of 4104 s (1.14 h). The digital recorded signals were low-pass filtered (4000 Hz cut-off frequency) and down-sampled by a factor of 3 to obtain the digital EEGs with sampling rate 14 700 Hz ($N = 10.05 \times 10^6$ samples for each ISI configuration). Eye-blink artifacts were suppressed with the iterative template matching and suppression (ITMS), an algorithm that detects, models, and suppresses blink-artifacts from a single-channel EEG (Valderrama *et al.*, 2018). Four subjects (aged 26–46 years) participated in this study. The protocol followed in this study was in accordance with the Code of Ethics of the World Medical Association (Declaration of Helsinki) for experiments involving humans, and it was approved by the Research Ethics Committee of the University Hospital "San Cecilio" of Granada (Spain).

The EEGs were processed with the conventional and the different matrix-based IRSA algorithms. The length of the response was set to 1 s ($J = 14\,700$ samples), in order to provide early, middle, and late evoked responses. The results of the different IRSA implementations were compared in two conditions: out of convergence (with a small convergence parameter and few iterations) and at convergence (with enough iterations).

B. Comparison of the IRSA results at a specific iteration

The results of the different IRSA implementations have been compared using a convergence parameter $\alpha = 0.02$ and 50 iterations. This convergence parameter was found to be small enough to avoid instability in the IRSA algorithm for all the ISI configurations. The responses estimated with so few iterations are out of convergence but this number of iterations allows a comparison of the resulting responses and the computational cost for the different implementations. The execution time was measured using a desktop computer with an Intel-Core i7-3770 CPU, 3.40 GHz, 8.00 GB RAM.

Table II shows a comparison of the different IRSA algorithms at 50 iterations. The results are the average for the four subjects included in the study. The responses provided by the different implementations have been compared using the SNR (defined as the ratio of the response energy to that of the difference between the compared responses, expressed in dB), where the responses provided by the conventional IRSA algorithm were used as a reference. An SNR around 260 dB indicates similar results up to the thirteenth significant digit, and an increment of 20 dB represents another decimal digit in accuracy. The high SNRs observed in the table support the mathematical equivalence of the different implementations. The small differences among the resulting responses are associated with the limited precision of the numerical representation and the propagation of small errors in the least significant digits in the numerical procedures.

Regarding the execution time, the computational efficiency of conventional-IRSA is poor, with a strong dependence on the ISI configuration. The matrix-IRSA substantially improves the efficiency and provides very stable execution times (as expected from the formulation). The optimization of the initialization leads to a slight improvement with respect to the matrix-IRSA algorithm. The FFT-based implementation of the matrix product provides the fastest algorithm. The RSLSD algorithm is the slowest one of the matrix-based implementations, due to the matrix division required in this algorithm. Detailed results, including the SNR and the execution time

TABLE I. Configuration of the AEP recording session. For each test: EEG duration $T = 684$ s; EEG length $N = 10.05 \times 10^6$ samples (sampling rate 14 700 Hz).

ISI range	Aver. stim. rate	K (stimuli)
480–960 ms	1.39 Hz	950
240–480 ms	2.78 Hz	1900
120–240 ms	5.56 Hz	3800
60–120 ms	11.11 Hz	7600
30–60 ms	22.22 Hz	15 200
15–30 ms	44.44 Hz	30 400

TABLE II. Comparison of the different IRSA algorithms at 50 iterations with $\alpha = 0.02$. The SNR evaluates the difference between the responses provided by the algorithms. The total execution time includes both the initialization and the iterations.

ISI (ms)	IRSA (convent)	IRSA (matrix)	IRSA (mat-opt)	IRSA (mat-FFT)	RSLSD (iterat.)
(a) SNR (dB) referred to IRSA-conventional responses					
480–960	—	309.7	312.7	308.5	278.0
240–480	—	308.4	310.4	308.0	271.9
120–240	—	307.2	308.6	307.4	264.4
60–120	—	304.2	305.1	306.3	261.7
30–60	—	300.4	301.0	303.9	256.7
15–30	—	297.6	298.0	300.7	253.4
Average	**—**	**304.6**	**306.0**	**305.8**	**264.3**
(b) Total execution time (s)					
480–960	17.99	17.83	12.35	0.69	27.9
240–480	33.3	17.54	12.75	1.11	28.7
120–240	63.7	17.54	13.52	1.89	29.2
60–120	125.0	17.22	15.19	3.41	31.7
30–60	245.4	16.84	17.52	6.26	34.8
15–30	485.1	16.61	21.8	10.58	37.5
All	**970.5**	**103.6**	**93.1**	**23.9**	**189.8**

(total, for initialization and per iteration), with mean and standard deviations, are provided in the supplementary material (section 11).[1] The responses obtained at 50 iterations are also included.

C. Comparison of the IRSA results at convergence

The convergence of the responses with the number of iterations has been studied using the fastest IRSA algorithm (IRSA-matrix-FFT), with $\alpha = 0.02$ and a number of iterations between 50 and 10 000. The results have been compared with those obtained with RSLSD (non iterative version), directly providing the results at convergence. The supplementary material[1] (section 12) contains results about the convergence of IRSA with the iterations, including the SNRs of the estimated responses (using those from RSLSD as reference) and the responses for one subject. This analysis shows (1) that the IRSA results tend to those at convergence as the number of iterations increases; (2) that numerical convergence (SNR > 260 dB) is obtained, with $\alpha = 0.02$ and 10 000 iterations, only at the 480–960 ms ISI condition; and (3) that a reasonable convergence (practical for audiological analysis of the responses) is guaranteed for SNR > 45 dB. For the experimental design of this study, $\alpha = 0.02$ and 10 000 iterations provide appropriate convergence (with SNR > 70 dB for all the ISI conditions).

Table III compares the results of the IRSA algorithms at convergence. Since all the iterative IRSA algorithms with fixed α are equivalent, results have been obtained only for the IRSA-matrix-FFT version (the fastest one), with $\alpha = 0.02$ and 10 000 iterations. The fast implementation of IRSA (including the selection of the optimum α and with convergence control) has been applied using 290 and 120 dB as convergence criterion (for numerical convergence and practical convergence, respectively). The RSLSD algorithm (direct estimation at convergence with matrix inversion) has also been applied. The responses provided by the different algorithms have been compared in terms of SNR using the RSLSD results as a reference, and the total execution time per subject has been measured for each algorithm and ISI condition. All the IRSA versions provide responses close enough to convergence. When α and the number of iterations are constant, the execution time moderately increases and the SNR strongly decreases with the stimulation rate. The fast implementation of IRSA benefits from the use of a specific convergence parameter for each ISI condition (the selected α increased from 0.0416 for ISI 15–30 ms to 0.8285 for ISI 480–960 ms), which provides the predefined convergence with the minimum number of iterations (the number of iterations decreased from 6300 to 34 between these ISI configurations for a convergence criterion of 120 dB). For the experimental conditions, the execution time of RSLSD is greater than those for the IRSA implementations (at all the ISI conditions) due to the computational complexity of the matrix division. Detailed results, including the SNR and the execution time (total, for initialization and per iteration), are provided in the supplementary material (section 13).[1] The selected convergence parameter and the number of iterations required for the fast implementations of IRSA, as well as the responses estimated using 120 dB as convergence criterion, are also included.

TABLE III. Comparison of the different IRSA algorithms at convergence. The SNR evaluates the difference between the responses provided by the algorithms. The total execution time includes both the initialization and the iterations.

ISI (ms)	IRSA (mat-FFT)	IRSA (fast-290 dB)	IRSA (fast-120 dB)	RSLSD (converg)
	(a) SNR (dB) referred to RSLSD-converg responses			
480–960	265.0	280.9	111.0	—
240–480	130.0	266.8	96.6	—
120–240	94.0	265.0	95.2	—
60–120	83.7	263.7	93.8	—
30–60	74.7	263.7	94.2	—
15–30	73.3	146.2	94.5	—
Average	**120.1**	**247.7**	**97.5**	—
	(b) Total execution time (s)			
480–960	17.30	0.81	0.69	23.6
240–480	17.61	2.71	1.59	24.6
120–240	18.37	6.23	3.35	24.8
60–120	20.1	12.21	6.35	26.5
30–60	23.1	24.7	12.76	29.6
15–30	28.2	31.3	24.0	34.9
All	**124.7**	**78.0**	**48.8**	**164.0**

D. Effect of the response length *J* over the execution time

In the previous analysis, the responses have been estimated with a response length $J = 14\,700$ (for a response duration of 1 s), because we are interested in the full-range AEPs including from brainstem to cortical responses. However, the execution time is strongly affected by the response length, and in a different way for the different implementations, since the computational complexity increases with J^2 for some ones and with $J \log_2(J)$ for others, and since the required number of iterations also depends on the convergence parameter (and therefore on the ISI configuration). In order to study the effect of the response length on the execution time, the IRSA implementations have been applied to the AEP experiment using response lengths between 147 samples (i.e., 10 ms) and 14 700 (1 s). The slow implementations of IRSA have been applied for 50 iterations and execution times are estimated for 10 000 iterations from those results. The IRSA-matrix-FFT implementation has been applied for 10 000 iterations. The fast IRSA implementation has been configured for 290 and 120 dB as convergence criterion, and the RSLSD (direct estimation at convergence) has also been applied. The results (total execution time per subject for all the ISI conditions as a function of the response length) are represented in Fig. 1. Detailed results (including the execution time and the estimated responses) are also shown in the supplementary material (section 14).[1]

The comparison of the computational cost at $J = 14\,700$ shows a prohibitive execution time for the conventional IRSA (2.23 days per subject). The matrix implementations (with and without optimization of the initialization) and the iterative RSLSD require similar execution times (around

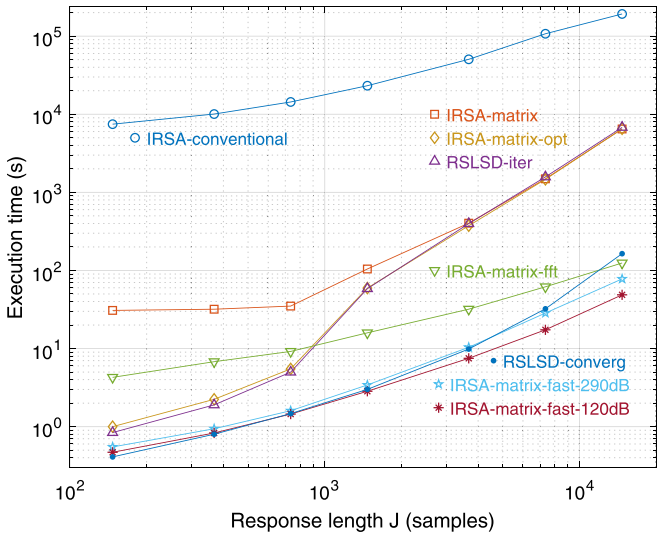

FIG. 1. (Color online) Total execution time of the IRSA/RSLSD algorithms for the complete experiment (all ISI conditions). Algorithms configured for convergence. Execution time per subject (average) as a function of the response length J.

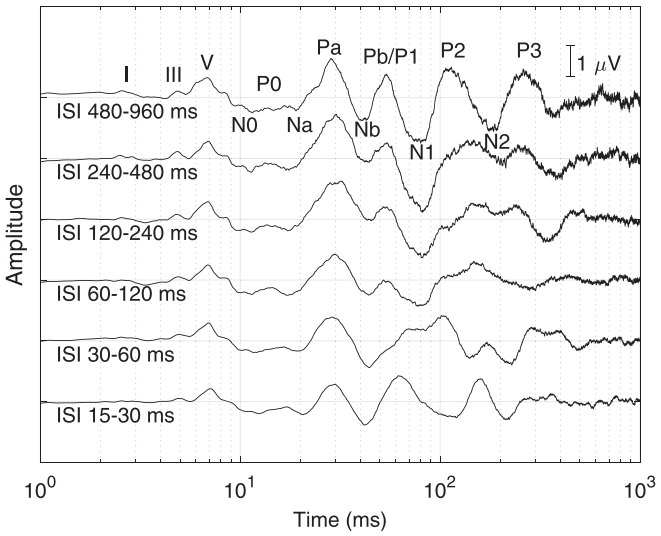

FIG. 2. Grand average of the AEP responses estimated with the fast matrix-based IRSA algorithm with 120 dB as convergence criterion.

1.8 h per subject) because most of the execution time is devoted to the iterations (because of matrix products). These execution times are significantly greater than those for the FFT or fast IRSA implementations or those of the direct RSLSD algorithm (which are between 48 s and 3 min).

As expected, the execution time decreases with the reduction of J in all the implementations. For the conventional IRSA, it is always too large (2.2 h for the shortest J). The evolution of the execution time of the matrix IRSA (with and without optimization in the initialization) reveals the utility of this optimization (very important when $J < 1000$). The similarity between the iterative RSLSD and the optimized matrix IRSA (and the differences between the conventional and iterative RSLSD) reveals that the iterative matrix product for 10 000 iterations takes more time than the matrix division of RSLSD. The FFT-based matrix product reduces the execution time for large J but the conventional matrix product is more efficient for $J < 1000$. Finally, the decrease of J reduces the computational cost of direct RSLSD more efficiently than the fast version of IRSA, being the execution time slightly shorter for small values of J (at $J = 147$, 0.41, and 0.47 s, respectively, for direct RSLSD and fast IRSA with 120 dB).

The responses estimated with different values of J are also represented in the supplementary material[1] (section 14) for one subject. Interestingly, the responses obtained with different values of J are not identical: the effect of reducing the response length is, approximately, a truncation of the response, but in addition to the truncation, some differences are clearly observed. These differences are associated with the number of degrees of freedom (in the response to be estimated) involved in the optimization problem.

E. Responses provided by IRSA

Figure 2 shows the responses provided by the fast IRSA algorithm with 120 dB as convergence criterion. These responses are the grand average estimated from the four subjects included in this study. The time axis is logarithmically scaled in order to clearly show the different evoked potentials, including three decades between 1 ms and 1 s. The waves of the evoked potentials are indicated in the plots, including auditory brainstem responses (ABR waves I, III, V), middle latency responses (MLR waves N_0, P_0, N_a, P_a, N_b, P_b), and cortical auditory evoked potentials (CAEP waves P_1, N_1, P_2, N_2, P_3). The different plots correspond to different ISI configurations, and some changes in the latency and amplitude of the waves can be appreciated as the stimulation rate increases.

The supplementary material[1] (section 15) includes details of the responses for each subject. In particular, each response (obtained with an EEG with a duration of 684 s) is compared with those obtained from three EEG portions of 228 s, (for consistency verification in the evoked responses). The supplementary material[1] (section 15) also includes a comparison of the grand average with the individual responses from each subject in order to provide an evaluation of the inter-individual differences.

IV. DISCUSSION AND CONCLUSIONS

This work presents a matrix formulation of the IRSA algorithm, which is mathematically equivalent to the conventional IRSA and is more efficient in terms of computational cost. Based on the matrix description, the convergence of the IRSA procedure has been analyzed. According to this analysis, the solution provided by IRSA can be rewritten as a geometric series of matrices, involving the autocorrelation matrix of the stimulation sequence R_s. This result has two interesting consequences. On one hand, the convergence criterion of the geometrical series provides a specific condition to be satisfied by the convergence parameter α in order to provide stability to the algorithm (and explains the instability observed when a too large α is selected). On the other hand, the analysis demonstrates that IRSA asymptotically

converges to the LS-deconvolution solution (Bardy *et al.*, 2014a; Bardy *et al.*, 2014b; Bardy *et al.*, 2014c).

The properties of the R_s matrix involved in the IRSA algorithm allow several optimizations: (i) FFT-based matrix product, (ii) selection of an optimal α based on the bound for the eigenvalues of R_s, (iii) optimization of the initialization, and (iv) control of convergence. These optimizations have been implemented in different versions of the algorithm.

The experimental results demonstrate the mathematical equivalence of the different IRSA implementations, as well as the mathematical equivalence of LS-deconvolution and IRSA at convergence. For the experimental design considered in this manuscript, the implementation of IRSA including all the proposed optimizations (IRSA-matrix-fast) is the most efficient one, even though RSLSD requires execution times not much longer. In addition, the fast implementation of IRSA requires neither the selection of the convergence parameter (since α is automatically selected from the bound for the eigenvalues) nor the number of iterations (since it is automatically controlled with the convergence criterion), which simplifies the configuration of the algorithm. This is relevant for the practical use of IRSA since the optimal configuration of these parameters strongly depends on the ISI configuration. The proposed optimizations allow the practical use of the IRSA method for many clinical and research applications, even for experimental designs involving long responses or ISI configurations requiring high overlapping of the responses (like the experiments reported in this study).

Beyond the computational efficiency, a significant contribution of the study is the formal demonstration of the equivalence of IRSA at convergence and LS-deconvolution. In this sense, this manuscript provides a unified formulation of both procedures. This perspective could be valuable for the interpretation of results in audiological studies using either IRSA or LS-deconvolution.

The matrix product required in IRSA can be performed with an FFT-based implementation because of the Toeplitz structure of the R_s matrix. This optimization is not possible in LS-deconvolution because this algorithm requires a matrix division that cannot be implemented with an FFT, in general, for Toeplitz matrices (an FFT-based matrix division would require the matrix to be circulant). In contrast, the FFT-based inversion is possible for the CLAD method (Ozdamar and Bohorquez, 2006), which can be considered a particular case of LS-deconvolution or IRSA methods where the stimulation sequence is periodically repeated (the periodicity of the stimulation sequence in CLAD forces the autocorrelation matrix R_s to be circulant, and therefore invertible with the FFT). In this sense, CLAD would provide a faster deconvolution (compared with IRSA or LS-deconvolution) even though it requires periodic stimulation sequences, which imposes limitations in the design of audiological experiments.

Regarding the audiological implication of the experimental results, the study presented in this manuscript shows that it is feasible to record all the components from the cochlea to the auditory cortex using clicks with a randomized interval presented at different stimulus rates. As originally proposed by Michelini *et al.* (1982), the representation of these signals in the logarithmic time scale facilitated the identification and labeling of the early-, middle-, and late-components.

The interest in obtaining brainstem and cortical neural activity simultaneously has existed for years. For example, Bidelman (2015), Krishnan (2012), and Slugocki *et al.* (2017) proposed different methods based on the combination of a transient cortical response and a steady-state brainstem response elicited by the same acoustic stimulus. The major drawback of these methods is that while the steady-state component provides an overall index of the neural salience at the brainstem, it does not allow the evaluation of the activity at each neural station (Krishnan, 2007), thus limiting the interpretation of the signal.

The morphology of the AEP signals shown in the present study is consistent with those reported by Holt and Ozdamar (2016) and Kohl *et al.* (2019). These studies used CLAD to deconvolve the full-range response from bursts of clicks and chirps presented at different rates (Holt and Ozdamar, 2016) and from an interleaved stimulus presentation paradigm consisting of bursts of clicks alternating with isolated clicks (Kohl *et al.*, 2019). However, only the wave V from the brainstem response could be evaluated in these studies. This could possibly be due to the presentation of the full-range AEP signal in the linear (rather than in the logarithmic) time scale in Holt and Ozdamar (2016), and to the narrow band-pass of the filter selected in Kohl *et al.* (2019), i.e., 1–750 Hz. In contrast, waves I, II, III, IV, V, and VII of the ABRs can be clearly identified in the grand-average signal, and in most of the subjects of the present study.

The representation of the full-range response in the logarithmic time scale presents a number of advantages compared with the traditional approach in which ABR, MLR, and CAEP components were obtained separately. First, it allows a comprehensive analysis of the ascending auditory pathway, in which all stations are synchronously evoked by the same stimulus. This could potentially be useful to evaluate interactions between central and peripheral neural activity, as well as a possible diagnostic tool for auditory neuropathy spectrum disorder (ANSD) since this population tends to show clear cortical, but absent brainstem components (Hood, 2007). Additionally, the proposed methodology may save testing time when both brainstem and cortical responses are relevant to the study since a single test would be required. Finally, the use of deconvolution overcomes the traditional limitation of EEG recordings in which the ISI had to be larger than the duration of the response in order to avoid overlapping responses. Deconvolution techniques are likely to play a relevant role in current research when evaluating how the human auditory system responds to more ecologically-valid stimuli, like real running speech (Valderrama *et al.*, 2019).

In order to provide the community with computational tools for deconvolving AEP responses, MATLAB/Octave code of the different IRSA and RSLSD implementations was included as supplementary material.[1] Additionally, a MATLAB/Octave script has been prepared for running simulations involving these tools (see the supplemental material, section 16).[1] The script reads an AEP response, synthesizes the EEG according to an experimental set-up and ISI configuration, and applies the different IRSA and RSLSD algorithms, providing the results

(estimated responses, comparison in terms of SNR and execution times). With this script, the user can recreate (in simulation) all the experiments included in this study or even under other experimental conditions. Additionally, we provide a compressed directory including the MATLAB/Octave functions, the script, and a file with a response to be used with the script for the simulations.

ACKNOWLEDGMENTS

This work was partially supported by the Spanish Ministry of Science, Innovation and Universities under the project EQC2018-004988-P. The authors acknowledge the constructive revision of the anonymous reviewers. In the authors' opinion, the manuscript has substantially improved with respect to the original draft thanks to the reviewer comments.

[1]See supplementary material at https://doi.org/10.1121/1.5139639 for a PDF file presenting (section 1) MATLAB/Octave code implementing the IRSA algorithm; (section 2) MATLAB/Octave code implementing the matrix IRSA algorithm; (section 3) detailed derivations of the IRSA solution expressed as a geometric series; (section 4) MATLAB/Octave code implementing the matrix IRSA algorithm with the optimized initialization; (section 5) detailed derivations of matrix product involving a Toeplitz matrix in the frequency domain; (section 6) MATLAB/Octave code for the FFT-based implementation of the matrix IRSA algorithm; (section 7) bounds for the eigenvalues of symmetric Toeplitz matrices and application for setting the convergence parameter; (section 8) MATLAB/Octave code implementing the fast version of the matrix IRSA algorithm (including the numerical accuracy checking, the optimized convergence parameter, the optimized initialization, and the FFT-based matrix product); (section 9) MATLAB/Octave code implementing the RSLSD algorithms at convergence (i.e., for infinite iterations); (section 10) MATLAB/Octave code implementing the RSLSD algorithms at a specified number of iterations; (section 11) detailed results of IRSA implementations at 50 iteration and $\alpha = 0.02$; (section 12) convergence analysis of the IRSA algorithm; (section 13) detailed results of the IRSA implementations at convergence; (section 14) execution time analysis in terms of the response length J; (section 15) individual AEP traces provided by IRSA; (section 16) MATLAB/Octave script for running simulations involving the different IRSA and RSLSD implementations. See also supplementary material for a compressed directory with scripts, functions, and examples in MATLAB/Octave aiming to help the reader implement the different versions of the IRSA and RSLSD algorithms described in this paper, and run simulations to replicate the results presented in this study.

Bardy, F., Dillon, H., and Dun, B. V. (**2014a**). "Least-squares deconvolution of evoked potentials and sequence optimization for multiple stimuli under low-jitter conditions," Clin. Neurophysiol. **125**, 727–737.

Bardy, F., Dun, B. V., Dillon, H., and Cowan, R. (**2014b**). "Least-squares (LS) deconvolution of a series of overlapping cortical auditory evoked potentials: A simulation and experimental study," J. Neural Eng. **11**, 046016.

Bardy, F., Dun, B. V., Dillon, H., and McMahon, C. M. (**2014c**). "Deconvolution of overlapping cortical auditory evoked potentials recorded using short stimulus onset-asynchrony ranges," Clin. Neurophysiol. **125**, 814–826.

Bidelman, G. M. (**2015**). "Towards an optimal paradigm for simultaneously recording cortical and brainstem auditory evoked potentials," J. Neurosci. Methods **241**, 94–100.

Bohorquez, J., and Ozdamar, O. (**2006**). "Signal to noise ratio analysis of maximum length sequence deconvolution of overlapping evoked potentials," J. Acoust. Soc. Am. **119**, 2881–2888.

Bohorquez, J., and Ozdamar, O. (**2008**). "Generation of the 40-Hz auditory steady-state response (ASSR) explained using convolution," Clin. Neurophysiol. **119**, 2598–2607.

Burkard, R. F., Finneran, J. J., and Mulsow, J. (**2018**). "Comparison of maximum length sequence and randomized stimulation and averaging methods on the bottlenose dolphin auditory brainstem response," J. Acoust. Soc. Am. **144**, 308–318.

Eysholdt, U., and Schreiner, C. (**1982**). "Maximum length sequences: A fast method for measuring brain-stem-evoked responses," Audiology **21**, 242–250.

Ferreira, P. (**1994**). "Localization of the eigenvalues of toeplitz matrices using additive decomposition, embedding in circulants, and the fourier transform," in *Proceedings of SysID'94, 10th IFAC Symposium on System Identification*, July 4–6, Copenhagen, Denmark.

Finneran, J. J. (**2017**). "Bottlenose dolphin (tursiops truncatus) auditory brainstem responses recorded using conventional and randomized stimulation and averaging," J. Acoust. Soc. Am. **142**, 1034–1042.

Finneran, J. J. (**2018**). "Conditioned attenuation of auditory brainstem responses in dolphins warned of an intense noise exposure: Temporal and spectral patterns," J. Acoust. Soc. Am. **143**, 795–810.

Finneran, J. J., Mulsow, J., and Burkard, R. F. (**2019**). "Signal-to-noise ratio of auditory brainstem responses (ABRs) across click rate in the bottlenose dolphin (tursiops truncatus)," J. Acoust. Soc. Am. **145**, 1143–1151.

Galambos, R., Makeig, S., and Talmachoff, P. J. (**1981**). "A 40-Hz auditory potential recorded from the human scalp," Proc. Natl. Acad. Sci. U.S.A. **78**, 2643–2647.

Gillespie, P. G., and Muller, U. (**2009**). "Mechanotransduction by hair cells: Models, molecules, and mechanisms," Cell **139**, 33–44.

Holt, F., and Ozdamar, O. (**2016**). "Effects of rate (0.3–40/s) on simultaneously recorded auditory brainstem, middle and late responses using deconvolution," Clin. Neurophysiol. **127**, 1589–1602.

Hood, L. J. (**2007**). "Auditory neuropathy and dys-synchrony," in *Auditory Evoked Potentials: Basic Principles and Clinical Application*, edited by R. Burkard, M. Don, and J. Eggermont (Lippincott Williams & Wilkins, Baltimore, MD), pp. 275–290.

Jewett, D. L., Caplovitz, G., Baird, B., Trumpis, M., Olson, M. P., and Larson-Prior, L. J. (**2004**). "The use of QSD (Q-sequence deconvolution) to recover superposed, transient evoked-responses," Clin. Neurophysiol. **115**, 2754–2775.

Kohl, M. C., Schebsdat, E., Schneider, E. N., Niehl, A., Strauss, D. J., Ozdamar, O., and Bohorquez, J. (**2019**). "Fast acquisition of full-range auditory event-related potentials using an interleaved deconvolution approach," J. Acoust. Soc. Am. **145**, 540–550.

Krishnan, A. (**2007**). "Frequency-following response," in *Auditory Evoked Potentials: Basic Principles and Clinical Application*, edited by R. Burkard, M. Don, and J. Eggermont (Lippincott Williams & Wilkins, Baltimore, MD), pp. 313–333.

Krishnan, A. (**2012**). "Relationship between brainstem, cortical and behavioural measures relevant to pitch salience in humans," Neuropsychologia **50**, 2849–2859.

Maddox, R. K., and Lee, A. K. C. (**2018**). "Auditory brainstem responses to continuous natural speech in human listeners," eNeuro **5**, e0441.

Michelini, S., Arslan, E., Prosser, S., and Pedrielli, F. (**1982**). "Logarithmic display of auditory evoked potentials," J. Biomed. Eng. **4**, 62–64.

Ozdamar, O., and Bohorquez, J. (**2006**). "Signal-to-noise ratio and frequency analysis of continuous loop averaging deconvolution (clad) of overlapping evoked potentials," J. Acoust. Soc. Am. **119**, 429–438.

Slugocki, C., Bosnyak, D., and Trainor, L. J. (**2017**). "Simultaneously-evoked auditory potentials (seaps): A new method for concurrent measurement of cortical and subcortical auditory-evoked activity," Hear. Res. **345**, 30–42.

Thornton, A. R. D. (**2007**). "Instrumentation and recording parameters," in *Auditory Evoked Potentials: Basic Principles and Clinical Application*, edited by R. Burkard, M. Don, and J. Eggermont (Lippincott Williams & Wilkins, Baltimore, MD), pp. 73–101.

Thornton, A. R. D., and Coleman, A. (**1975**). "The adaptation of cochlear and brainstem auditory evoked potentials in humans," Electroencephalogr. Clin. Neurophysiol. **39**, 399–406.

Thornton, A. R. D., and Slaven, A. (**1993**). "Auditory brainstem responses recorded at fast stimulation rates using maximum length sequences," Br. J. Audiol. **27**, 205–210.

Valderrama, J. T., Alvarez, I., de la Torre, A., Segura, J. C., Sainz, M., and Vargas, J. L. (**2012**). "Recording of auditory brainstem response at high stimulation rates using randomized stimulation and averaging," J. Acoust. Soc. Am. **132**, 3856–3865.

Valderrama, J. T., de la Torre, A., Alvarez, I., Segura, J. C., Sainz, M., and Vargas, J. L. (**2013**). "A portable, modular, and low cost auditory brainstem response recording system including an algorithm for automatic identification of responses suitable for hearing screening," in *Proceedings of the IEEE/EMBS Special Topic Conference on Point-of-Care HealthCare Technologies (PoCHT)*, January 16–18, Bangalore, India, pp. 180–189.

Valderrama, J. T., de la Torre, A., Alvarez, I., Segura, J. C., Sainz, M., and Vargas, J. L. (**2014a**). "A flexible and inexpensive high-performance auditory evoked response recording system appropriate for research purposes," Biomed. Eng./Biomed. Technik **59**, 447–459.

Valderrama, J. T., de la Torre, A., Alvarez, I., Segura, J. C., Thornton, A. R. D., Sainz, M., and Vargas, J. L. (**2014b**). "Auditory brainstem and middle latency responses recorded at fast rates with randomized stimulation," J. Acoust. Soc. Am. **136**, 3233–3248.

Valderrama, J. T., de la Torre, A., Alvarez, I., Segura, J. C., Thornton, A. R. D., Sainz, M., and Vargas, J. L. (**2014c**). "A study of adaptation mechanisms based on abr recorded at high stimulation rate," Clinical Neurophysiology **125**, 805–813.

Valderrama, J. T., de la Torre, A., and Dun, B. V. (**2018**). "An automatic algorithm for blink-artifact suppression based on iterative template matching: Application to single channel recording of cortical auditory evoked potentials," J. Neural Eng. **15**(1), 016008.

Valderrama, J. T., de la Torre, A., Dun, B. V., and Segura, J. C. (**2019**). "Towards the recording of brainstem and cortical evoked potentials from the fine structure of natural speech," in *Proceedings of the XXVI International Evoked Response Audiometry Study Group (IERASG) Biennial Symposium*, June 30–July 4, Sydney, Australia.

Valderrama, J. T., de la Torre, A., Medina, C., Segura, J. C., and Thornton, A. R. D. (**2016**). "Selective processing of auditory evoked responses with iterative-randomized stimulation and averaging: A strategy for evaluating the time-invariant assumption," Hear. Res. **333**, 66–76.

Woldorff, M. G. (**1993**). "Distortion of ERP averages due to overlap from temporally adjacent ERPs: Analysis and correction," Psychophysiology **30**, 98–119.